Quantum criticality in the cubic heavy-fermion system CeIn3−xSnx

R. Küchler, Philipp Gegenwart, J. Custers, O. Stockert, N. Caroca-Canales, C. Geibel, J. G. Sereni, F. Steglich

Quantum Criticality in the Cubic Heavy-Fermion System CeIn$_{3-x}$Sn$_x$

R. Küchler,[1] P. Gegenwart,[1] J. Custers,[1] O. Stockert,[1] N. Caroca-Canales,[1] C. Geibel,[1] J. G. Sereni,[2] and F. Steglich[1]

[1]*Max-Planck Institute for Chemical Physics of Solids, D-01187 Dresden, Germany*
[2]*Laboratorio Bajas Temperaturas, Centro Atomico Bariloche, 8400 S.C. Bariloche, Argentina*
(Received 1 February 2006; published 30 June 2006)

We report a comprehensive study of CeIn$_{3-x}$Sn$_x$ ($0.55 \leq x \leq 0.8$) single crystals close to the antiferromagnetic quantum-critical point (QCP) at $x_c \approx 0.67$ by means of the low-temperature thermal expansion and Grüneisen parameter. This system represents the first example for a *cubic* heavy fermion in which T_N can be suppressed *continuously* down to $T = 0$. A characteristic sign change of the Grüneisen parameter between the antiferromagnetic and paramagnetic states indicates the accumulation of entropy close to the QCP. The observed quantum-critical behavior is compatible with the predictions of the itinerant theory for three-dimensional critical spin fluctuations. This has important implications for the role of the dimensionality in heavy-fermion QCPs.

Non-Fermi-liquid (NFL) properties are observed in many heavy-fermion (HF) systems and frequently attributed to a nearby quantum-critical point (QCP) [1]. A QCP can arise by continuously suppressing the transition temperature T_N of an antiferromagnetic (AF) phase to zero, e.g., by chemical or applied pressure or an external magnetic field. QCPs are of great current interest due to their singular ability to influence the finite temperature properties of materials. Heavy-fermion metals have played the key role in the study of AF QCPs. The essential question is how the heavy quasiparticles evolve if these materials are tuned from the paramagnetic into the AF ordered state. The traditional picture describes a spin-density-wave (SDW) transition and related, a mean-field type of quantum-critical behavior. Here the quasiparticles retain their itinerant character [2,3]. Unconventional quantum criticality, which qualitatively differs from the standard theory of the $T = 0$ SDW transition, may arise due to a destruction of Kondo screening. Here the quasiparticles break up into their components: conduction electrons and local $4f$ moments forming magnetic order [4,5]. This locally critical picture leads to a number of distinct properties, including stronger than logarithmic mass divergence, ω/T scaling in the dynamical susceptibility, and a large reconstruction of the Fermi surface. Such behavior has been found at least in some HF systems [6–8]. The central question is to identify the crucial parameter leading to the different types of QCPs. Of particular importance should be the dimensionality of the magnetic fluctuations, which could be reduced by the presence of frustration. It is proposed in Ref. [4] that for magnetically three-dimensional (3D) systems without frustration the itinerant SDW picture should apply. On the other hand, 2D magnetic systems should be described by a locally quantum-critical picture [4]. However, systems currently under investigation are either tetragonal, e.g., CeNi$_2$Ge$_2$, YbRh$_2$(Si$_{1-x}$Ge$_x$)$_2$ [9], and CeCu$_2$Si$_2$ [10], hexagonal, e.g., YbAgGe [11], or monoclinic, e.g., CeCu$_{6-x}$Au$_x$ [6], and the lower crystallographic symmetry

could result in fluctuations with reduced dimensionality. Therefore, the dimensionality of the critical spin fluctuations clearly needs to be substantiated by inelastic neutron scattering experiments. In order to avoid this constraint, experiments on cubic systems close to QCPs are particular interesting. CeIn$_{3-x}$Sn$_x$, with a cubic point symmetry of Ce atoms in the Cu$_3$Au structure (compare the inset in Fig. 1), is thus an excellent candidate for such a study, as here low-dimensional spin fluctuations can be ruled out. Thus, the interesting question arises whether the mechanism of NFL behavior in this system can be described by an itinerant 3D-SDW theory.

In this Letter, we present thermal-expansion measurements and a Grüneisen ratio analysis performed on single-crystalline samples of the cubic system CeIn$_{3-x}$Sn$_x$ close to the critical concentration $x_c = 0.67$, where T_N is suppressed to zero by doping. Recently, it has been shown that the thermal volume expansion $\beta = V^{-1}(dV/dT)$ (V: sample volume) is particularly suited to probe quantum-critical behavior, since, compared to the specific heat, it is much more singular in the approach to the QCP [12]. As a consequence, the Grüneisen ratio $\Gamma \sim \beta/C$ of thermal expansion $\beta(T)$ to specific heat $C(T)$ is divergent as T goes to zero at any pressure-sensitive QCP, and the associated critical exponent can be used to distinguish between the different types of QCPs. In the itinerant scenario, the divergence $\Gamma \propto 1/T^\epsilon$ is given by $\epsilon = 1/\nu z$ [12], with ν the critical exponent for the correlation length $\xi \propto |r|^\nu$ (r: distance from the QCP) and z the dynamical critical exponent in the divergence of the correlation time $\tau_c \propto \xi^z$. For a 3D AF QCP, $\nu = 1/2$ and $z = 2$, yielding $\epsilon = 1$. Thus, a study of the Grüneisen ratio can prove the validity of the 3D-SDW picture in the title system provided that $\epsilon = 1$.

The magnetic (x, T) phase diagram of polycrystalline CeIn$_{3-x}$Sn$_x$ has been widely studied for $0 \leq x \leq 1$ by susceptibility [13], specific-heat [14], and resistivity measurements [15,16] (see Fig. 1). Whereas T_N for undoped
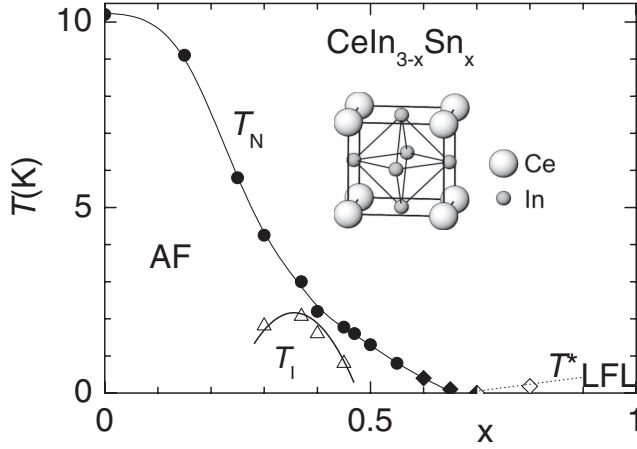
FIG. 1. Magnetic phase diagram for cubic CeIn$_{3-x}$Sn$_x$ ($x \leq$ 1). The solid circles and diamonds indicate T_N, determined from specific-heat [14] and electrical resisitivity [15] measurements, respectively. The open diamonds mark $T^\star$, the upper limit of Landau Fermi-liquid behavior, e.g., $\Delta\rho(T) \propto T^2$ [16]. The open triangles indicate first-order transition T_I [14].

CeIn$_3$ vanishes discontinuously below 3 K under hydrostatic pressure [17], it can be traced down to 0.1 K for CeIn$_{3-x}$Sn$_x$, and an additional first-order phase transition T_I has been found for $0.25 < x < 0.5$ inside the AF state [14]. These differences are related to the change of the electronic structure induced by Sn doping. Beyond a possible tetracritical point at $x \approx 0.4$ [14], an almost linear dependence of $T_N(x)$ is observed. This is in contrast to $T_N \propto (x_c - x)^{2/3}$ predicted by the 3D-SDW theory [2]. Thus, the origin of the NFL behavior in this system remains an open question, and further thermodynamic studies are needed to shed light on the nature of the QCP.

The CeIn$_{3-x}$Sn$_x$ single crystals investigated here ($0.55 \leq x \leq 0.80$) were grown by a Bridgman-type technique. Large single crystals with a mass of 15 g were produced, analyzed by x-ray powder diffraction, and found to be of single phase with the proper cubic structure. Within the $\pm 2\%$ accuracy of the x-ray diffraction, no impurity phases were resolvable. Thin bars with a length $2 \leq l \leq 6$ mm, suitable for the dilatometric investigations, were cut out. The thermal expansion has been measured in a dilution refrigerator using an ultrahigh resolution capacitive dilatometer with a maximum sensitivity corresponding to $\Delta l / l = 10^{-11}$.

Figure 2(a) shows the volume thermal expansion β of single-crystalline CeIn$_{3-x}$Sn$_x$ with $x = 0.55, 0.65, 0.7,$ and 0.8 plotted as $\beta(T)/T$ vs $\log T$. The volume-expansion coefficient β is given by $\beta = 3 \times \alpha$, with α being the linear thermal-expansion coefficient. For $x = 0.55$, the broadened steplike decrease in β/T at $T_N \approx 0.6$ K marks the AF phase transition, in perfect agreement with specific-heat measurements on the same single crystal [18]. Upon increasing the concentration, we find for $x = 0.65$ and 0.7 diverging behavior over nearly two decades in T down to
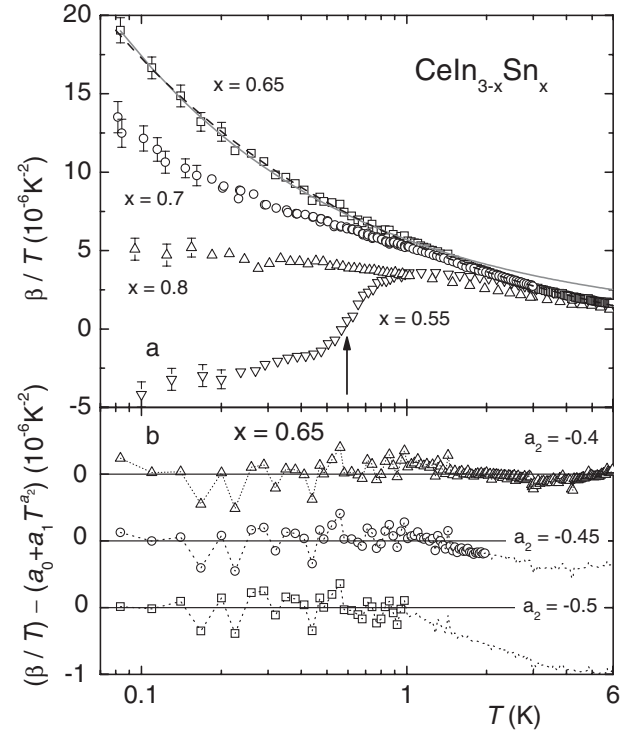

FIG. 2. (a) Volume thermal-expansion coefficient β of CeIn$_{3-x}$Sn$_x$ single crystals as β/T vs $\log T$. The gray solid and black dashed lines indicate $T^{-0.5}$ and $T^{-0.4}$ dependencies, respectively. The arrow indicates AF phase transition. (b) Deviation of β/T data for a $x = 0.65$ sample from best power-law fits for $T \leq 1$ K (squares), $T \leq 2$ K (circles), and $T \leq 6$ K (triangles), respectively, as $(\beta/T) - (a_0 + a_1 T^{a_2})$ vs $\log T$. For clarity, the three data sets have been shifted by different amounts vertically.

80 mK. These data suggest that T_N is suppressed at a critical concentration $x_c \approx 0.67 \pm 0.03$, also consistent with specific-heat measurements performed on the same samples [18]. Finally, for $x = 0.8$ we recover Fermi-liquid behavior $\beta(T)/T \approx$ const for $T \rightarrow 0$.

In the following, we will analyze the observed NFL behavior and make a comparison with the predictions of the itinerant SDW scenario [12]. A best-fit description of the $x = 0.65$ data in the entire temperature range 0.08 K $\leq T \leq 6$ K according to $\beta/T = a_0 + a_1 T^{a_2}$ reveals $a_2 = -0.4 \pm 0.01$ [see the dashed line in Fig. 2(a)]. However, as shown in the upper part of Fig. 2(b), the deviation between the data and this fit shows several broad bumps, indicating that the fit does not properly describe the data. We therefore tried best power-law fits for 0.08 K $\leq T \leq T_{max}$ with varying T_{max}. For $T_{max} = 1$ K, the fit is of excellent quality [cf. solid line in Fig. 2(a) and lowest part of Fig. 2(b)] and the resulting exponent equals -0.5, i.e., the value predicted by the 3D-SDW scenario [12].

We now turn to the Grüneisen parameter defined as $\Gamma = (V_m/\kappa_T)(\beta/C)$, where the constants V_m and κ_T denote the molar volume and isothermal compressibility, respectively.

The specific heat has been studied in the temperature range $40\ mK \leq T \leq 4\ K$ on the same $CeIn_{3-x}Sn_x$ samples used for thermal expansion [18,19]. Here the nuclear quadrupole contribution of indium which becomes important below 150 mK has been subtracted. Figure 3 shows a comparison of $\Gamma(T)$ for all samples studied in thermal expansion. Since the temperature dependence of specific heat is much weaker compared to that of thermal expansion, its influence to the Grüneisen parameter is rather small. Therefore, the variation of $\Gamma(T)$ for the different $CeIn_{3-x}Sn_x$ samples is very similar to that found in β/T (compare Fig. 2). Both single crystals closest to x_c, $x = 0.65$ and $x = 0.7$, show a divergent behavior down to the lowest accessible temperature with very large Γ values at 0.1 K which are of similar size as found for other quantum-critical HF systems [9,20]. On the other hand, saturation is observed for $x = 0.55$ and $x = 0.8$ being located in the AF ordered and the Fermi-liquid regime, respectively. The fact that the divergence of $\Gamma(T)$ in the quantum-critical regime is stronger than logarithmic (compare the double-logarithmic representation of the $x = 0.65$ data presented in the inset in Fig. 3) provides clear evidence for a well defined (pressure-sensitive) QCP in the system. If the disorder present in the system would lead to a "smeared" quantum-critical regime, $\Gamma(T)$ could diverge at most logarithmically [12].

Another indication for a QCP is the sign change of the Grüneisen parameter between the ordered and the disordered regime. As discussed in Ref. [21], it is directly
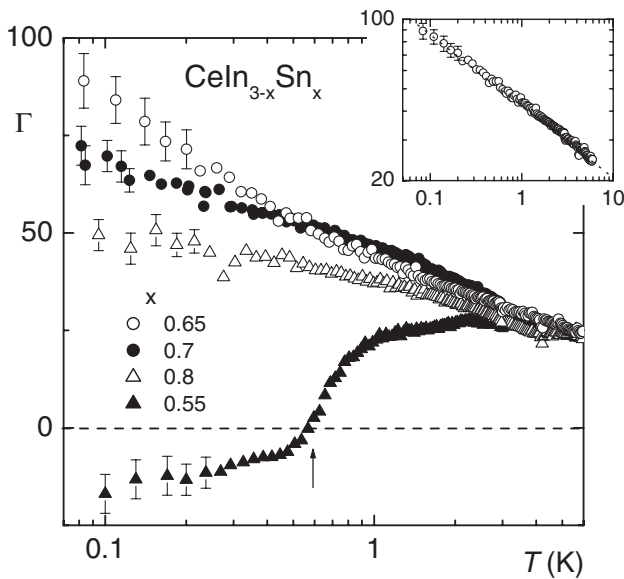

FIG. 3. Temperature dependence of the Grüneisen parameter $\Gamma = (V_m/\kappa_T)(\beta/C)$ of several $CeIn_{3-x}Sn_x$ single crystals as $\Gamma(T)$ vs $\log T$. $V_m = 6.25 \times 10^{-5}\ m^3\,mol^{-1}$ and $\kappa_T = 1.49 \times 10^{-11}\ Pa^{-1}$ [26] are the molar volume and isothermal compressibility, respectively. The arrow indicates AF phase transition. The inset displays data for $x = 0.65$ in a double-logarithmic plot. The dotted line indicates the power-law dependence $\Gamma \propto T^{-0.31}$.

related to the entropy accumulation near the QCP. The different signs of Γ in the AF and paramagnetic regions reflect the opposite pressure dependencies of the respective characteristic energy scales. Below T_N, the effective AF intersite interaction dominates, whose negative pressure dependence gives rise to a negative Grüneisen parameter $\Gamma < 0$. On the other hand, the positive Grüneisen ratio in the paramagnetic state is compatible with the positive pressure dependence of the Kondo temperature in Ce-based HF systems.

In order to compare our results for the $x = 0.65$ sample which is located closest to the QCP with the theoretical predictions for an itinerant AF QCP [12], we need to calculate the *critical* Grüneisen ratio $\Gamma^{cr}(T) \propto \beta^{cr}/C^{cr}$ of critical contributions to thermal expansion and specific heat. For thermal expansion, $\beta^{cr}(T) = \beta(T) - a_0 T$, with $a_0 = 0.3 \times 10^{-6}\ K^{-2}$ as determined from the best fit up to 1 K; see above. Within the itinerant theory for the 3D AF case, the critical contribution to specific heat is *subleading* [12]: $C^{cr}(T) = C(T) - \gamma_0 T$, with $C^{cr} < 0$, $C^{cr}/T \to 0$ for $T \to 0$, and $\gamma_0 = C/T|_{T=0}$. For γ_0, we use the value $0.851\ Jmol^{-1}\,K^{-2}$ obtained in Ref. [18] from fitting the low-temperature electronic specific heat in a *restricted* temperature range $0.3\ K \leq T \leq 1.4\ K$ according to $C/T = \gamma_0(1 - a'\sqrt{T})$. Figure 3 displays a log-log plot of $\Gamma^{cr}(T)$ versus temperature. We find $\Gamma^{cr} \propto T^{-\epsilon}$, with an exponent $\epsilon = 1.1 \pm 0.1$ which is very close to 1, predicted by the itinerant theory. Note that this exponent is rather insensitive of γ_0 subtracted from the specific-heat data: Using $\gamma_0 = 0.9$ and $0.95\ Jmol^{-1}\,K^{-2}$ results in $\epsilon = 1.07$ and 1.02, respectively. Interestingly, the exponent for the critical Grüneisen ratio, which theoretically equals the dimension of the most relevant operator that is coupled to pressure [12], holds over a much larger temperature range than the respective 3D-SDW dependencies in specific heat [18] and thermal expansion (cf. Fig. 2). A similar observation has also been made for $CeNi_2Ge_2$ [9].

For those two systems for which an unconventional QCP has been proposed, $YbRh_2Si_2$ and $CeCu_{6-x}M_x$ ($M = Au$, Ag), distinctly different temperature dependences have been observed: $\Gamma^{cr} \propto T^{-0.7}$ in the former [9] and $\Gamma^{cr} \propto \log T$ [20] in the latter case. It is proposed in Ref. [4] that for magnetically 3D systems without frustration the SDW picture should apply. This is consistent with our Grüneisen ratio analysis.

For the 3D AF case, the itinerant theory predicts an *asymptotic* $T^{3/2}$ dependence for the temperature dependent part to the electrical resistivity [2,3]. As discussed in Ref. [22], the interplay between strongly anisotropic scattering due to the critical spin fluctuations and isotropic impurity scattering can lead at *elevated temperature* to temperature exponents of the resistivity between 1 and 1.5, depending on the amount of disorder. Systematic $\rho(T)$ studies down to mK temperatures on polycrystalline $CeIn_{3-x}Sn_x$ revealed an almost linear temperature depen-
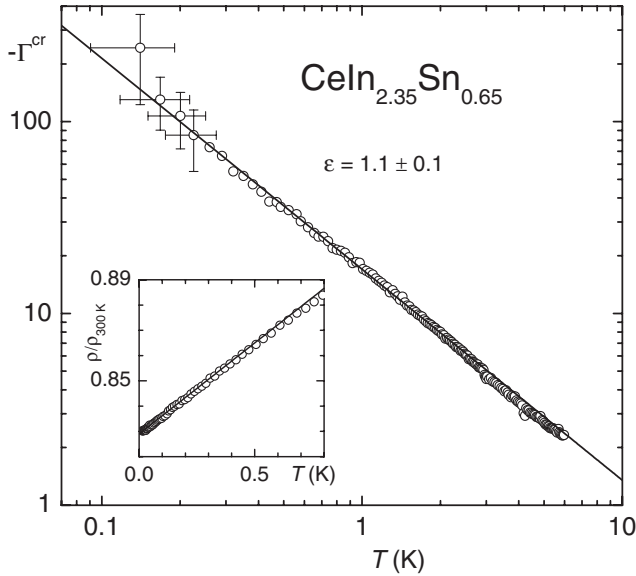
FIG. 4. Critical Grüneisen ratio $\Gamma^{cr} = (V_m/\kappa_T)(\beta^{cr}/C^{cr})$ for CeIn$_{2.35}$Sn$_{0.65}$ as logΓ^{cr} vs log$T$ with critical components $\beta^{cr} = \beta(T) - a_0 T$ and $C^{cr} = C(T) - \gamma T$ derived after subtraction of background contributions (see text). The solid line represents $\Gamma^{cr} \propto 1/T^\epsilon$, with $\epsilon = 1.1 \pm 0.1$. The inset shows the low-temperature electrical resistivity of a single crystal of similar composition.

dence in the quantum-critical regime [15]. Similar behavior is observed for single-crystalline CeIn$_{2.35}$Sn$_{0.65}$ as well; see the inset in Fig. 4. However, due to the high Sn doping needed to tune the system towards the QCP, the resistivity ratio $\rho_{300\,K}/\rho_0$ is of the order of 1 and the temperature variation amounts to a few percent of ρ_0 only, making the comparison with theoretical predictions very difficult. This indicates that transport experiments alone are not sufficient to characterize quantum criticality in disordered systems. Possibly, also the slope of $T_N(x)$ differs from the 3D-SDW prediction because disorder is not constant but increases with increasing x. However, the algebraic divergence of $\Gamma(T)$ for $T \rightarrow 0$ at $x \approx x_c$ proves a pressure-sensitive QCP in the system and excludes disorder-driven scenarios for the observed NFL behavior [12].

In conclusion, our study on CeIn$_{3-x}$Sn$_x$ single crystals by means of the low-temperature thermal expansion and Grüneisen parameter has proven the applicability of the itinerant theory for 3D critical spin fluctuations in this cubic system. Since strong contradictions to this theory have been found in systems such as CeCu$_{5.9}$Au$_{0.1}$ [6] or YbRh$_2$(Si$_{1-x}$Ge$_x$)$_2$ [7] with lower crystallographic symmetry and, at least in the case of the former system, strongly anisotropic quantum-critical fluctuations, the parameter *dimensionality* obviously plays an important role for the nature of HF QCPs. We tentatively classify the

different HF systems studied by Grüneisen analysis at their respective QCPs as follows: (i) CeIn$_{3-x}$Sn$_x$ and CeNi$_2$Ge$_2$ [9], for which the latter system neutron scattering measurements revealed 3D low-energy magnetic fluctuations [23], show thermodynamic behavior compatible with the 3D itinerant theory, whereas for (ii) YbRh$_2$(Si$_{1-x}$Ge$_x$)$_2$ [9] and CeCu$_{5.8}$Ag$_{0.2}$ [20] strong contradictions to this model (for both 2D and 3D critical spin fluctuations) are observed. Neutron scattering has proven 2D quantum-critical fluctuations in CeCu$_{5.9}$Au$_{0.1}$ [24], while for YbRh$_2$Si$_2$ a complicated behavior with competing AF and ferromagnetic quantum-critical fluctuations has been observed [25]. The comparison with our results on CeIn$_{3-x}$Sn$_x$ suggests that a destruction of Kondo screening causing unconventional quantum criticality is prevented in magnetically 3D systems.

[1] See, e.g., S. Sachdev, *Quantum Phase Transitions* (Cambridge University Press, Cambridge, England, 1999).
[2] A. J. Millis, Phys. Rev. B **48**, 7183 (1993).
[3] T. Moriya and T. Takimoto, J. Phys. Soc. Jpn. **64**, 960 (1995).
[4] Q. Si *et al.*, Nature (London) **413**, 804 (2001).
[5] P. Coleman and C. Pépin, Physica (Amsterdam) **312B–313B**, 383 (2002).
[6] A. Schröder *et al.*, Nature (London) **407**, 351 (2000).
[7] J. Custers *et al.*, Nature (London) **424**, 524 (2003).
[8] S. Paschen *et al.*, Nature (London) **432**, 881 (2004).
[9] R. Küchler *et al.*, Phys. Rev. Lett. **91**, 066405 (2003).
[10] P. Gegenwart *et al.*, Phys. Rev. Lett. **81**, 1501 (1998).
[11] S. L. Bud'ko, E. Morosan, and P. C. Canfield, Phys. Rev. B **69**, 014415 (2004).
[12] L. Zhu *et al.*, Phys. Rev. Lett. **91**, 066404 (2003).
[13] J. Lawrence, Phys. Rev. B **20**, 3770 (1979).
[14] P. Pedrazzini *et al.*, Eur. Phys. J. B **38**, 445 (2004).
[15] J. Custers *et al.*, Acta Phys. Pol. B **34**, 379 (2003).
[16] J. Custers, Ph.D. thesis, Technische Universität Dresden, 2003 (unpublished).
[17] N. D. Mathur *et al.*, Nature (London) **394**, 39 (1998).
[18] T. Rus *et al.*, Physica (Amsterdam) **359B–361B**, 62 (2005).
[19] T. Radu (née Rus), Ph.D. thesis, Technische Universität Dresden, 2005 (unpublished).
[20] R. Küchler *et al.*, Phys. Rev. Lett. **93**, 096402 (2004).
[21] M. Garst and A. Rosch, Phys. Rev. B **72**, 205129 (2005).
[22] A. Rosch, Phys. Rev. Lett. **82**, 4280 (1999).
[23] H. Kadowaki *et al.*, Phys. Rev. B **68**, 140402(R) (2003).
[24] O. Stockert *et al.*, Phys. Rev. Lett. **80**, 5627 (1998).
[25] K. Ishida *et al.*, Phys. Rev. Lett. **89**, 107202 (2002).
[26] I. Vedel *et al.*, J. Phys. F **17**, 849 (1987).